Long-Term Corrosion Investigation of CoCrMoW Alloys under Simulated Physiological Conditions

Loredana Preda , Sorina-Alexandra Leau , Cristina Donath , Elena Ionela Neacsu , Monica Elisabeta Maxim , Veronica Sătulu , Alexandru Paraschiv , Maria Marcu *

Posted Date: 10 October 2023

doi: 10.20944/preprints202310.0638.v1

Keywords: corrosion; CoCr-based alloy; passive film biomaterials

Article

Long-Term Corrosion Investigation of CoCrMoW Alloys under Simulated Physiological Conditions

Loredana Preda [1,*], Sorina Alexandra Leau [1], Cristina Donath [1], Elena Ionela Neacsu [1], Monica Elisabeta Maxim [1], Veronica Satulu [2], Alexandru Paraschiv [3] and Maria Marcu [1,*]

[1] Institute of Physical Chemistry "Ilie Murgulescu", Splaiul Independentei 202, 060021, Bucharest, Romania; loredana@icf.ro; sleau@icf.ro; cdonath@icf.ro; eneacsu@icf.ro; mmaxim@icf.ro; m_marcu@icf.ro

[2] National Institute for Laser, Plasma and Radiation Physics, Atomistilor 409, Magurele, 077125, Romania; veronica.satulu@inflpr.ro

[3] COMOTI—Romanian Research Development Institute for Gas Turbines, Iuliu Maniu Bd. 220D, 061126, Bucharest, Romania; alexandru.paraschiv@comoti.ro

* Correspondence: M. M. m_marcu@icf.ro ; L. P. loredana@icf.ro

Abstract: The corrosion resistance of two cast CoCr based alloys, with different amounts of chromium and with different alloying elements in the bulk composition of the alloy, was assessed. Herewith, we investigated the corrosion behavior of Co21Cr8Mo7W and Co29Cr7W by open circuit potential (OCP), potentiodynamic polarization (PP) and electrochemical impedance spectroscopy (EIS) in 0.1 M phosphate buffer solution (PBS) at 37°C for long time immersion. After 1000 hours of immersion, the corrosion current density (i_{cor}), estimated from anodic polarization tests, is lower for Co21Cr8Mo7W (i.e. 49 nA cm^{-2}) alloy compared to Co29Cr7W alloy (180 nA cm^{-2}). As regards the corrosion potential (E_{cor}), a nobler value was observed for Co21Cr8Mo7W (i.e. -59 mV vs. Ag/AgCl) compared to Co29Cr7W (i.e. -114 mV vs. Ag/AgCl). These findings suggest a better corrosion resistance of the film formed on the alloy containing lower amount of Cr and two alloying elements, namely Mo and W. These results are promising ones in terms of medical applications because they open new strategies in obtaining alloys with lower content of chromium and with higher protective properties against corrosion attack.

Keywords: corrosion; CoCr-based alloy; passive film; biomaterials.

1. Introduction

CoCr along with titanium alloys are the most frequently used materials in surgical implant applications, chiefly for hard tissue replacement [1,2]. The use of the CoCr based alloys as biomaterial, attracts a lot of attention because of their excellent properties such as high corrosion resistance, good biocompatibility and good mechanical properties [3, 4]. Among the properties required for using these materials for surgical applications, a very good corrosion resistance of the alloy is a mandatory one.

The corrosion resistance of these biomaterials is influenced by several factors like, the alloy itself (e.g. chemical composition, microstructure, surface state), the characteristics of the environment (pH, temperature), as well as the way of manufacturing these biomaterials [5,6]. For instance, by casting method, alloys with very good corrosion resistance were obtained compared to those ones where a manufacturing method was employed [7,8]. As regards the environment, for example, it was reported that the corrosion resistance of Co28Cr6Mo alloys is drastically reduced when these alloys are tested in NaCl compared to PBS [9] his behavior most probably is related to the fact that in such aggressive media the ion chlorides are attacking the protective film formed on the surface, leading to the pitting corrosion processes and finally to the film dissolution. Conversely, in PBS media, this type of alloy is less exposed to corrosion attack because during the immersion period, the phosphate ions adsorbed on the surface act as a efficient barrier between the alloy and environment [9,10].

As many studies revealed, the corrosion behavior of these types of alloys is drastically influenced by the chemical composition of the alloy as well. In this respect, a lot of research work is devoted [11,12]. For example, at Co29Cr alloy, a good resistance to corrosion attack was observed in SBF simulated biofluid [13] because a film, containing significant amount of Cr_2O_3 and small amounts of cobalt oxides, is formed [14]. It is well accepted that mainly the presence of Cr_2O_3 and/ or Co $(OH)_3$ species in the film plays a key role in providing good corrosion protection of these CoCr-based alloys. However, at long-time immersion in similar media (e.g. artificial saliva, Ringer solution and Hank solution), dissolution processes at interface alloy/biofluid are noticed, yielding to a notable instability of the film [12,14]. In order to answer to these issues, many approaches were tackled over the time and, recently, data attested that the addition of a small amount of molybdenum in the composition of the CoCr alloy is about to obtain films with conspicuous protective properties. As the electrochemical corrosion tests evidenced, the Mo itself stabilizes the passive film. These reported data opened new perspectives in finding other pathways for obtaining alloys with very good corrosion resistance. Other attempts were reported over the time, as manufacturing CoCr-based alloys with small amounts of W. For these CoCrW alloys, it was observed, that the addition W does not bring about a better stability of the film and rather a superior mechanical property of the alloy which does not necessarily improve corrosion resistance of the material [15].

As result, in the last few years, molybdenum (Mo) and tungsten (W) were added as alloying elements in CoCr-based alloys and promising outcomes were obtained. At these new alloys, the improved corrosion resistance emerges actually from the synergetic effect of Mo, W and Cr which promotes the formation of a compact passive film with good stability [11,16,17] which indeed acts like a barrier between the alloy surface and the biofluid, impeding hence the dissolution of the metallic elements [18]. In other words, Mo and W provide benefits towards passivation and protective role in the breakdown processes, yielding resistance to corrosion attack and hence to the dissolution of the film [17].

Concerning other aspects of using these CoCr based alloys for medical applications, their costs should be envisaged, and especially those ones related to chromium. In this respect, new gates were opened by means of manufacturing CoCr based alloys with lower content of Cr. However, by reducing the amount of Cr, the corrosion resistance of material is most probably diminished with undesirable consequences in their use for medical applications. Therefore, to reduce the content of Cr and at the same time to have CoCr-based alloys with good corrosion resistance, the addition of Mo and Was alloying elements is a valuable option. No literature data about the corrosion behavior of these new types of alloys, i.e. Co Cr MoW in biofluids were reported. Most frequently studies are devoted for corrosion behavior of CoCr, CoCrMo or CoCrMoW alloys with high amount of chromium (e.g 27-30 % Chromium) [11,19,20].

Herewith, we studied the corrosion behavior of two types of alloys with different concentrations in Cr and with different alloying elements as W and Mo. These studies are actually aimed at opening new perspectives in finding strategies for obtaining alloys, with low content of Cr and with excellent corrosion behavior. The evidence of the role played by alloying elements in the corrosion behavior of these CoCr-based alloys is another goal of this research work. Thus, the corrosion behavior of two types of alloys after long term immersion period, i.e. 1000 hours, were studied in PBS solution by electrochemical methods (i.e. open circuit potential (OCP), potentiodynamic polarization (PP) and electrochemical impedance spectroscopy (EIS)) The first alloy contains a high amount of Cr (29 % Cr) and as alloying element W, labeled Co29Cr7W, whereas the second one contains a lower amount of Cr (21 %) and as alloying elements Mo and W ones, labeled Co21Cr8Mo7W. In order to better understand the corrosion behavior of these alloys, additional information will be gained mainly from X-ray photoelectron spectroscopy (XPS) and inductively coupled plasma mass spectroscopy (ICP) techniques. In our opinion, by studying the corrosion behavior of these alloys after long term immersion instead of short ones, very often reported in literature, added value is brought to the study because more accurate information about their corrosion behavior is gained.

Preprints (www.preprints.org) | NOT PEER-REVIEWED | Posted: 10 October 2023 doi:10.20944/preprints202310.0638.v1

2. Materials and Methods

Co21Cr8Mo7W and Co29Cr7W alloys were tested in the form of rods with 8 mm in diameter. The chemical composition of these alloys, in cast state, is presented in Table 1.

Table 1. Chemical composition (% wt. and standard error) of the main components of Co21Cr8Mo7W and Co29Cr7W alloys.

Sample	% Co	% Cr
Co21Cr8Mo7W	64 ± 0.54	21 ± 0.32
Co29Cr7W	64 ± 0.52	29 ± 0.35

Before experiments, the samples were mechanically prepared by grinding with abrasive paper and suspensions of micrometric alumina powder, up to the metallographic quality, then degreased in ethanol in an ultrasonic bath and rinsed with distilled water.

The experiments were performed in a 0.1 M phosphate buffer saline solution (PBS) with the following composition: 8 gL^{-1} NaCl, 0.2 gL^{-1} KCl, 1.44 $gL^{-1}Na_2HPO_4$ and 0.25 gL^{-1} KH_2PO_4. The solution was maintained at a pH= 7.4 and a temperature of 37°C. All reagents were analytical grade (Sigma-Aldrich), and the solution was prepared using bidistilled water.

2.1. Electrochemical Measurements

The open-circuit potential was monitored during 1000 hours of immersion, at 37°C in natural aerated solutions, and the potential values are related to Ag/AgCl reference electrode. Three identical samples of 1 cm^2 were immersed in a 50 mL PBS solution in a Thermocal 20 incubator. At predetermined time intervals the stationary potentials were measured in open circuit (OCP). After different periods of immersion (168 and 1000 hours) the Tafel curves were recorded, in a potential range of 250 mV vs. Ag/AgCl around the corrosion potential, with a rate of 2.5 mV s^{-1} to evaluate the corrosion rate of specimens. At the same time the EIS data acquired potentiostatic at rest potential, between 1MHz and 10^{-2} Hz, with a perturbation of 10 mV. At the end of the immersion period, the anodic polarization curves were acquired between -300 mV and + 1000 mV with a potential sweep rate of 2.5 mVs^{-1}. All electrochemical measurements were performed using a PARSTAT 4000 potentiostat/galvanostat in a three-electrode electrochemical cell with a platinum sheet as counter electrode, Ag/AgCl as a reference electrode and the samples as working electrode. The acquired data were processed using the CorrView 3.3d and the Zview 2.70 dedicated software. To certify the reproducibility, three identical samples of each alloy (Co21Cr8Mo7W and Co29Cr7W) were tested.

2.2. Surface Characterization and Electrolyte Analysis

The surface chemical composition of these alloys was investigated by *X-ray Photoelectron Spectroscopy* (XPS) using an Escalab Xi+ system from Thermo Scientific provided with Al Ka gun. Acquisition steps of 1 eV and 0.1 eV were used for general spectra and high-resolution spectra, respectively. The deconvolution of high-resolution spectra was performed by Thermo Scientific Avantage Software. The C1s line at 284.4 eV was used as a reference to correct the binding energies for charge energy shift. A Shirley background was subtracted from the spectra. Least-square curve-fitting of the spectra was performed based on a mixture of Gaussian –Lorentzian functions.

The changes in hydrophobicity of the surface because of corrosion products depositions were highlighted by wetting analysis. *The contact angle measurement* was done with Drop Shape Analysis System apparatus, 133 DSA1 model (FM40 Easy Drop) from KRÜSS GmbH Germany. The samples were placed on a plane support and drops of deionized water with a volume of 3 µL each were put on the surface with a dispensing micro-syringe. The contact angle values were collected in static regime at room temperature, initially and at 30 seconds after the drop of water was placed on the sample surface. Static contact angle was recorded using Sessile Drop Fitting method for the angles in between 30–90° and Circle Fitting method for those less than 30°. Over 7 measurements were averaged for each sample.

Preprints (www.preprints.org) | NOT PEER-REVIEWED | Posted: 10 October 2023 doi:10.20944/preprints202310.0638.v1

The chemical analysis of electrolyte after 168 hours of immersion was performed using an inductively coupled plasma optical emission spectrometer with axial and radial viewing plasma configuration (ICP-OES, Optima 2100 DV Perkin Elmer), operating at a 40 MHz free-running ratio-frequency. For each extraction environment, two blank samples are measured as a reference.

3. Results and Discussions

3.1. Electrochemical Evaluation of CoCrMoW Alloy

The electrochemical characterization of Co21Cr8Mo7W and Co29Cr8Mo7W samples was carried out in order to analyze the corrosion behavior of these alloys in PBS.

3.1.1. OCP evolution

Figure 1 presents the overtime monitoring of the OCP for both alloys immersed in PBS solution during 1000 hours at 37°C. The evolution of the OCP with time is almost the same for both samples. During the first 24 hours, the initial potentials increase significantly with an approximative rate of 7.7 mV h^{-1}(up to +50 mV for Co21Cr8Mo7W and -50 mV for Co29Cr7W), indicating the spontaneous formation of a protective layer on surface materials in the biofluid. At both samples, between 24 and 230 hours of immersion, the OCP values are changing with time, suggesting that some processes of adsorption or/and dissolution occur at the interface, leading inevitably to both surface composition changes and apparently a slight instability of the protective layer. According to literature data [21, 22] among the possible processes of adsorption/dissolution that could occur at the interface, the adsorption of the phosphate ions on the alloy surface (mainly as chromium and cobalt phosphate complexes (e.g. $Co(H_2PO_4)_2$) followed by their partial dissolution might not be disregarded. As other reports suggest [9,21,23], by the formation of these chromium and cobalt phosphate species on the surface, the corrosion attack might be mitigated. Indeed, in our case this phenomenon is observed. Thus, as Figure 1 illustrates, it was noticed that the OCP values remain approximately constant between 230 and 1000 hours, revealing that during this period of immersion, the layer formed on both samples becomes a stable one with protective properties against the corrosion processes. However, the OCP values of Co21Cr8Mo7W alloy are situated at more positive potentials compared to those ones of Co29Cr7W alloy, i.e. a shift of 100 mV, regardless the immersion period (Figure 1). One may infer that the protective layer formed on the surface of Co21Cr8Mo7W hampers better the further dissolution of the alloys and increases the corrosion resistance of the material [13].

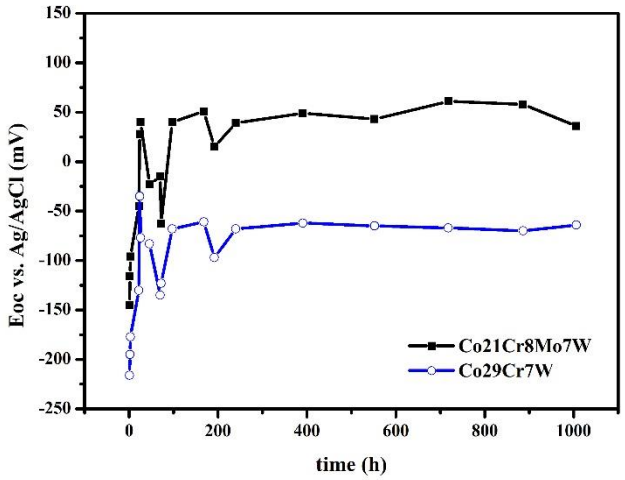

Figure 1. OCP evolution of Co21Cr8Mo7W and Co29Cr7W alloys in 0.1 M PBS solution during 1000 hours of immersion at 37°C.

Preprints (www.preprints.org) | NOT PEER-REVIEWED | Posted: 10 October 2023 doi:10.20944/preprints202310.0638.v1

3.1.2. Anodic Polarization

In order to find out more information about corrosion behavior of both samples, after 1000 hours of immersion in PBS, the Tafel plots and potentiodynamic polarization curves were recorded and they are exhibited in Figure 2. From polarization curves, at both samples, a current density (j) less than 10 μA cm^{-2} was observed in a potential range of about 630 mV (Figure 2). These results attest that both samples have a comparable passive domain in which the film formed on surface protects the surface against corrosion attack. These findings appear to attest that both samples can be used successfully for biomaterial applications, because the potential domain, in which the dissolution of oxide layer is obstructed, is actually large. For other CoCrMo alloys, a similar domain passivation was evidenced [9,10,21]. Literature reports attested that the resistance to passive dissolution of CoCr based alloys is mainly due to the formation of **chromium oxide** and **cobalt and chromium phosphate complexes** [10,20,22] on the surface. Given that the chemical composition of our samples is not too different from that of these CoCrMo alloys already studied, one may presume that a similar phenomenon takes place in our case. After 0.6 V vs. Ag/AgCl, a transpassive domain is observed, regardless of the type of specimen, revealing that at surface of both samples, a dissolution of the film starts to occur. One may presume that the attack of the surface after 0.6 V, in this neutral environment, is most probably mainly due to both the dissolution of chromium oxide and phosphate chromium ion complexes formed on the surface and water oxidation [10]. The existence of a transpassive domain after 0.6 V was also reported for other cast cobalt chromium alloys [9,24]. However, as Figure 2 illustrates, in the transpassive domain, a slight increase of the current density (j) is noticed for Co21Cr8Mo7W samples, i.e. from 10 μA cm^{-2} to 43 μA cm^{-2}, whereas, for Co29Cr7W samples, a sudden increase of the current density, i.e. from 10 μA cm^{-2} to 550 μA cm^{-2} is observed. **This behavior points out clearly that the layer formed on Co21Cr8Mo7W surface has better protective properties against the corrosion attack and is more stable**. At first sight, this demeanor appears to be surprising, because the Co29Cr7W alloy, which has a higher amount of chromium compared to Co21Cr8Mo7W (Table 1) has a slightly lower corrosion resistance. In most cases, for different cast CoCrMo alloys [11,25], the presence of a high amount of chromium, mainly as Cr_2O_3, provides inhibiting properties of the surface to corrosion processes. Based on these observations, we assume that, in our case, not necessary the presence of a higher amount of Cr in the alloy brings about a better stability of the film and rather the synergetic effect of Cr, Mo and W present in the alloy composition prevents the corrosion attack most probably due to the formation of a very stable and compact layer on their surface. Since at other CoCrMo alloys, it was observed that the presence of Mo facilitates the formation of a compact and stable chromium oxide film, our findings appear not to be quite unexpected [16,17].

In order to have a better insight about the corrosion behavior of these alloys in perspective of using them in medical fields, the ion release investigations were performed at both samples after 168 hours of immersion according to ISO 10271:2001 [26]. The results, shown in the Table 3, reveals a significant quantity of chromium ion released at Co29Cr7W, i.e. 73.7 μg cm^{-2} compared to Co21Cr8Mo7W where a negligible amount of chromium ions is released, i.e. 0.15 μg cm^{-2}.

These results are of great importance in terms of medical applications of these types of alloys, because they clearly attest that only the Co21Cr8Mo7W is suited for surgical implants, (i.e 0.15 μg cm^{-2} concentration of chromium ion released) because the concentration of chromium ion released is much lower than that worldwide accepted. (i.e. maximum 0.5 μg cm^{-2} [27]).

Moreover, as a higher amount of chromium ions, mainly associated with the dissolution of chromium oxide or chromium hydroxide from the passive film, is observed to be released at Co29Cr7W compared to Co21Cr8Mo7W, the less stability of the film at Co29Cr7W is hence expected to be noticed.

This corrosion behavior of our CoCrMoW alloys deserves to be further in detail investigated to clearly certify that Co21Cr8Mo7W is more appropriate for biomaterial applications and to elucidate the main factors responsible for such behavior.

Better protective properties of the film formed on Co21Cr8Mo7W against corrosion processes is also clearly evidenced from the corrosion parameters (Table 2), estimated from Tafel plots (inset

Preprints (www.preprints.org) | NOT PEER-REVIEWED | Posted: 10 October 2023 doi:10.20944/preprints202310.0638.v1

Figure 2). Therefore, the corrosion potentials (E_{cor}), determined after two different period of immersion, are situated at more positive potentials (Table 3) at Co21Cr8Mo7W, i.e. -0.061 V and -0.059 V at 168 and 1000 hours of immersion for Co21Cr8Mo7W and -0.104 V and -0.114 V for Co29Cr7W at same periods of immersion. Furthermore, the corrosion current density (j_{cor}), appraised, after the same periods of immersion, is lower (Table 3) at Co21Cr8Mo7W, i.e. 0.038 μA cm^{-2} and 0.049 μA cm^{-2} at Co21Cr8Mo7W and 0.427 μA cm^{-2} and 0.180 μA cm^{-2} at Co29Cr7W. As expected, a similar trend was observed for the evolution of corrosion rate, measured at the same periods of immersion, where slower corrosion rates were observed at Co21Cr8Mo7W, i.e. 1.09 μm y^{-1} and 2.81 μm y^{-1}. From these results, it is also interesting to notice that the corrosion parameters of Co21Cr8Mo7W, i.e. E_{cor}, i_{cor} and corrosion rates, are not notably changing with immersion time, revealing that the protective film formed on CoCrMoW alloy remains stable. One may conclude that the Co21Cr8Mo7W has better corrosion resistance and is more appropriate for surgical applications.

In terms of medical applications, another property of these materials which should not be disregarded is the hydrophobic/hydrophilic character effected by the protective film formed on the surface of the samples. Therefore, static contact angle measurements were carried out before and after 1000 hours of immersion at both specimens. The results revealed that at both types of samples, the character of the samples surface is changed from a hydrophobic one before the immersion (i.e. 99.33 ± 0.5 dgr for Co21Cr8Mo7W and 98.93 ± 0.5 dgr for Co29Cr7W) to a hydrophilic one after the immersion (i.e. 69.87 ± 0.5 dgr for Co21Cr8Mo7W and 67.79 ± 0.5 dgr for Co29Cr7W), suggesting that actually the protective film formed on both types of alloys has a hydrophilic character. Therefore, the evidence of the formation of a stable layer on these alloys, with hydrophilic character which both inhibits corrosive attack and provides good affinity for the adhesion of the cells, might open new reliable perspectives in obtaining CoCrMoW alloys with conspicuous properties for medical implants.

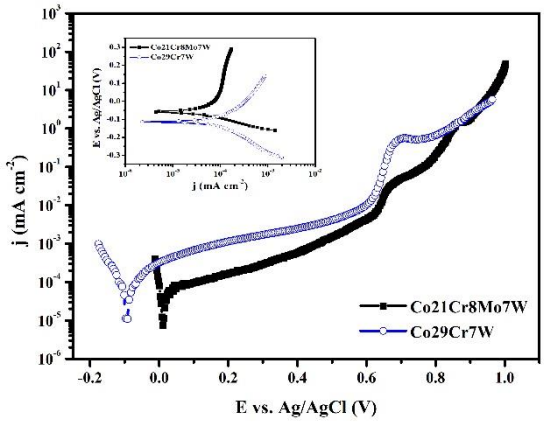

Figure 2. Polarization curves of Co21Cr8Mo7W and Co29Cr7W alloys after 1000 h of immersion in PBS solution at 37°C. In set: Tafel plots on Co21Cr8Mo7W and Co29Cr7W alloys after 1000 h of immersion.

Table 2. Corrosion parameters of Co21Cr8Mo7W and Co29Cr7W alloys. after immersion in 0.1M PBS at 37°C.

Sample	$i_{cor.}$ (μA cm^{-2})		E_{cor} vs. Ag/AgCl (mV)		Corrosion rate (μm y^{-1})	
	168 h	1000 h	168 h	1000 h	168 h	1000 h
Co21Cr8Mo7W	0.038	0.049	-61	-59	1.09	2.81
Co29Cr7W	0.427	0.180	-104	-114	12.24	6.57

Preprints (www.preprints.org) | NOT PEER-REVIEWED | Posted: 10 October 2023 doi:10.20944/preprints202310.0638.v1

Table 3. Ions released of Co21Cr8Mo7W and Co29Cr7W alloys after 168 hours immersion in 0.1M PBS at 37°C.

Sample	Metal element	Quantity of ions released	
		(mg L^{-1})	(µg cm^{-2})
Co21Cr8Mo7W	Co	0.679 mg/L	7.1
	Cr	< 0.02 mg/L	0.15
	Mo	21.8 µg/L	0.22
	W	undetectable	
Co29Cr7W	Co	0.335 mg/L	3.33
	Cr	7.40 mg/L	73.7
	W	undetectable	

3.2. Electrochemical Impedance Spectroscopy

Additional information about the corrosion behavior of both types of samples were obtained from the EIS investigations, carried out potentiostatically at OCP, after 1000 hours of immersion in PBS solution.

As Figure 3a illustrates, within the frequency range from 0.01 to 10^5 Hz, the impedance Z is much higher at Co21Cr8Mo7W compared to Co29Cr7W, suggesting that the oxide film formed on Co21Cr8Mo7W exhibits better protective properties against the corrosion processes. These findings are in good agreement with previous ones from anodic polarization investigations which attested a similar corrosion behavior at both samples.

In order to gain further information about the corrosion behavior of these samples, by considering an equivalent circuit (EEC) with two time constant in series (Figure 3b, inset), the impedance spectra of both specimens (Figure 3) were fitted. By using this EEC, the experimental data gave the best fit. The first time constant, constituted from CPE_{in}/R_{in}, is attributed to the oxide layer formed, during the immersion, on the surface and the second time constant, constituted from CPE_{out}/R_{out}, accounts for the dissolution processes at interface alloy/electrolyte and the inhomogeneity of the passive film. Due to these physical complex phenomena and heterogeneity of the surface, the constant phase elements (CPE_{out} and CPE_{in}) instead of capacitances were more adequate for fitting the EIS spectra [28], and the chi -squared values (X^2) are lower than 1.3E-3 for both samples. This EEC was previously successfully used for describing corrosion behavior of other CoCrMo alloys in different media [9,10,12]. The values of the equivalent circuit parameters of both alloys in the PBS solution are shown in Table 4.

From these parameters, the polarization resistance (R_p) of both specimens, calculated as the sum of R_{out} and R_{in}, was estimated and they are 8.6×10^6 Ω cm^2 and 2.3×10^6 Ω cm^2 for Co21Cr8Mo7W and Co29Cr7W respectively. As the R_p values of both samples are of the order of Megaohms, it appears that the film formed on both specimens have good corrosion resistance and, from this perspective, they can be further used for surgical applications. However, the R_p of Co21Cr8Mo7W alloy is cca. four times higher than that one of Co29Cr7W alloy, suggesting that a more stable oxide film with better resistance corrosion is formed on Co21Cr8Mo7W. These results are in good agreement with electrochemical corrosion investigations which attested better corrosion performance at Co21Cr8Mo7W alloy and a lower rate of passive layer dissolution (Table 2). These findings are supported by the results obtained for the inner resistances, R_{in}, of both samples which seems to attest a similar trend evolution (Table 4). The EIS results point out clearly that Co21Cr8Mo7W alloy has better surface protection.

Preprints (www.preprints.org) | NOT PEER-REVIEWED | Posted: 10 October 2023 doi:10.20944/preprints202310.0638.v1

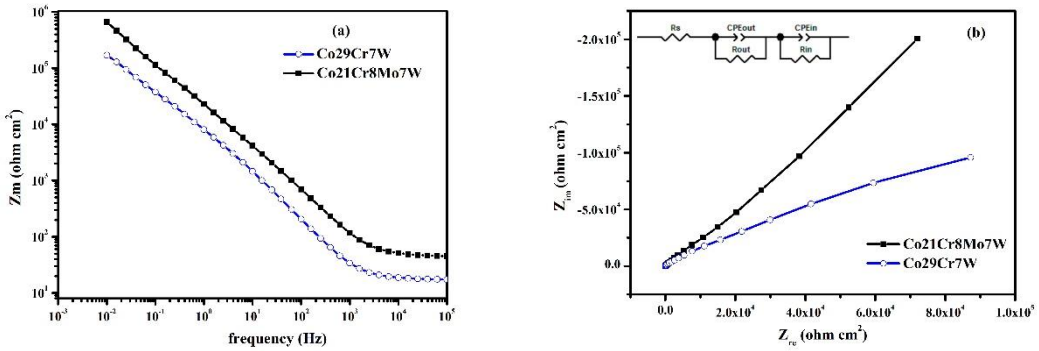

Figure 3. Bode plots (a) and Nyquist diagrams (b) of Co21Cr8Mo7W and Co29Cr7W alloys. after 1000 h of immersion in PBS at 37°C.

Table 4. EIS parameters obtained from fitting experimental data on the proposed equivalent electrical circuit of Co21Cr8Mo7W and Co29Cr7W alloys after 1000 hours immersion in 0.1M PBS at 37°C.

Sample	Rs (Ω cm^2)	CPE$_{out}$ ($S^n\ \Omega^{-1}$ cm^{-2})	n	R$_{out}$ (Ω cm^2)	CPE$_{in}$ ($S^n\ \Omega^{-1}$ cm^{-2})	n	R$_{in}$ (Ω cm^2)
Co21Cr8Mo7W	15.78	5.63×10^{-5}	0.80	6461	3.85×10^{-5}	0.81	8.6×10^{6}
Co29Cr7W	17.01	3.63×10^{-5}	0.86	7540	4.36×10^{-5}	0.84	2.3×10^{6}

3.3. X-ray Photoelectron Spectroscopy Investigations

The surface chemical composition of Co21Cr8Mo7W and Co29Cr7W alloys was investigated by XPS after their immersion in PBS solution at 37°C for 1000 hours. The XPS analysis attested mainly the presence of cobalt, chrome, tungsten, oxygen, phosphorus on the surface of both specimens. Besides, on the Co21Cr8Mo7W surface, molybdenum is evidenced. These results are in line with those from chemical composition (Table 1) which revealed the presence of the cobalt, chromium, tungsten elements in the bulk of both types of alloys and molybdenum only in the Co21Cr8Mo7W bulk alloy.

Based on literature reports [9,13] and our findings which revealed the presence of a certain amount of phosphorus (i.e. cca. 18 %) on the surface of both specimens, one may assume that during immersion, a non -negligible amount of cobalt and chromium phosphate complexes (e.g. $Co(H_2PO_4)_2$) are formed on the surface.The presence of these adsorbed complexes on the protective film formed on alloys, as electrochemical results suggest, is expected to mitigate the corrosion attack, and hence to have a certain contribution in ensuring a large passivation domain of both alloys, i.e. about 630mV.

In order to go deeper in understanding the corrosion behavior of these alloys, the Cr 2p, W 4f, Mo 3d, and O 1s deconvoluted high resolution spectra were recorded and the deconvoluted high resolution spectra of both alloys are shown in Figures 4 and 5.

The Cr-2p$_{3/2}$ spectra of both types of alloys were fitted with 5 peaks (Figures 4a and 5a). These peaks are attributed to chromium metallic species (Cr^0) (BE 547.5 ± 0.2 eV, [13,18]) Cr (III) oxide most probably present as Cr_2O_3 species (BE = 575.7 ± 0.2 eV, [13, 16]), $Cr(OH)_3$ species (BE 576.9 ± 0.2 eV, [13,16]), chromium mixed oxide species (BE 578.2 ± 0.2 eV, [29]) and Cr (VI) oxide, like CrO_3 species (BE 579.5 ± 0.2 eV, [23]). The corresponding relative fractions of the chemical species are shown in inset of figures. From deconvoluted Cr-2p$_{3/2}$ spectra one may assert that a significant amount of Cr_2O_3 and $Cr(OH)_3$ species are formed on the surface of both specimens. It is well known that the presence of these constituents in the passive film ensures good protective properties of the film against corrosion attack [9,13,16]. Thus, based on these findings, one may presume that, good protective properties of the film formed on the surface of both alloys is due to the presence of these non-negligible amounts of chromium oxide and chromium hydroxide species in the film. However, a higher concentration of Cr_2O_3 and $Cr(OH)_3$ species is present in the passive film formed on the

 doi:10.20944/preprints202310.0638.v1

Co29Cr7W surface (i.e. Cr_2O_3 20.29 % and $Cr(OH)_3$ 30.90 %) compared to Co21Cr8Mo7W (i.e. Cr_2O_3 14.91 % and $Cr(OH)_3$ 28.52 %). These results along with those from electrochemical investigations appear to reveal that the presence of a higher amount of Cr_2O_3 and chromium hydroxide species in the film not necessary brings about better protective properties of the film against corrosion processes. Therefore, in order to better explain the raison behind the corrosion behavior of these alloys, further XPS analysis was necessary to be achieved.

The W-4f spectra of Co21Cr8Mo7W were deconvoluted by assuming one doublet associated to WO_3 species (the W $4f_{7/2}$ of this doublet is at BE 35.9 eV ± 0.2 eV, [30,31]) (Figure 4b) and that one of Co29Cr7W (Figure 5b) was deconvoluted by assuming three doublets attributed to W^0 species (the W $4f_{7/2}$ of the first doublet is at BE 31.4 ± 0.2 eV, [30,31]), W^{5+} species (the W $4f_{7/2}$ of the second doublet is at BE 34.9 ± 0.2 eV, [32]) and WO_3 species (the W $4f_{7/2}$ of the third doublet is at BE 36 ± 0.2 eV [30,31]). For each doublet we considered a spin orbit splitting of 2.1 eV and a W $4f_{7/2}$ / W $4f_{5/2}$ ratio of 1.33 [32]. The corresponding relative fractions of the chemical species are shown in insets of the corresponding figures. These results clearly point out that the tungsten constituent in the protective film formed on Co21Cr8Mo7W surface is only present as tungsten (VI) oxide species, whereas on Co29Cr7W surface, is also present as W metallic and W^{5+} species.

As regards the Mo 3d spectrum of Co21Cr8Mo7W, this spectrum was deconvoluted by considering one double associated to MoO_3 species (the Mo $3d_{5/2}$ of this doublet is at 232.7 ± 0.2 eV, [22,29]) (Figure 4c). For this doublet we considered a spin orbit splitting of 3.13 eV and a Mo $3d_{5/2}$ / Mo $3d_{3/2}$ ratio of 0.67 [29]. It is obvious from these results that molybdenum constituent in the film is present only as MoO_3.

In summary, from the above XPS investigations and literature data [11,18,20], one may conjecture that in fact good corrosion resistance observed at Co29Cr7W alloys originate from the presence of both chromium species (i.e. Cr_2O_3 and $Cr(OH)_3$) in a significant amount and tungsten oxides species in a much lower amount in the passive film. Conversely at Co21Cr8Mo7W, the XPS results correlated with reported data [16,17, 19], revealed that good corrosion behavior of this alloy is mainly due to the synergetic effect of Cr, W and Mo present in the film as Cr_2O_3, $Cr(OH)_3$, WO_3 and MoO_3. Previous data from literature revealed that better corrosion resistance of the film formed on CoCr-based alloys surface might be gained when Mo and W are incorporated as alloying elements. The MoO_x and WO_3 species present in the passive film seem to ensure a good compactness of the film [33]. Other reports [16] demonstrated that an efficient barrier against the diffusion of species through the film formed on the surface of these types of alloys might be obtained when both the MoO_2 /similar products and the WO_3 are present in the protective oxide film. It was also evidenced that these oxide species were contributing to the sluggishness of the selective dissolution process of the metals beneath them.

As a conclusion, based on XPS results and electrochemical outcomes, one may emphasize that better corrosion performance observed at Co21Cr8Mo7W alloy is strongly related to the synergetic effect of Cr, W and Mo and cannot be hence disregarded.

These observations are conspicuous ones because they point out that indeed the presence of Cr in a higher amount in the alloy (i.e. 29 % for Co29Cr7W and 21 % for Co21Cr8Mo7W) not necessary hampers very well the corrosion processes (i.e. r_{cor} is 2.81 μm y^{-1} for Co29Cr7W and 1.09 μm y^{-1} for Co21Cr8Mo7W) and actually the synergetic effect of Cr, Mo and W constituents present in the passive film as oxides is responsible for excellent protective properties of the film against corrosion attack. In other words, one may conjecture that, in our case, at Co21Cr8Mo7W, the presence of W as only hexavalent tungsten oxide along with the presence of molybdenum as MoO_3 in the film brings about improved protectiveness properties of the passive film, impeding hence better the dissolution processes in the film. Besides, Cwalina K.L. et all. [17] demonstrated that the presence of WO_3 species in the passive film extend the passive range because the stability of the film is enhanced by means of interaction of W with water, which leads to the formation of insoluble WO_3 phase. Thus, we consider that the extended passive range and lowered passive current density observed at Co21Cr8Mo7W alloy (i.e. ΔE_{pass} = 0.63 V; i_{pass} = 0.4 μA cm^{-2}) compared to Co29Cr7W alloy (ΔE_{pass} =

Preprints (www.preprints.org) | NOT PEER-REVIEWED | Posted: 10 October 2023 doi:10.20944/preprints202310.0638.v1

0.49 V; i_{pass} = 1.2 μA cm^{-2}) is also due to the presence of a higher amount of WO_3 species in the passive film formed on Co21Cr8Mo7W surface (Figures 4b and 5b).

The O-1s spectra of both types of alloys, deconvoluted with three peaks, associated to $O^{metal-oxide}$ species (BE 530.4 ± 0.2 eV, [9, 13]), hydroxide or hydroxyl groups, OH^- (BE 531.7 ± 0.2 eV, [34]) and to chemisorbed water (BE = 532.8 ± 0.3 eV, [34] and/or metal-PO_4 [23], (Figures 4d and 5c) support our above XPS results which attested manly the presence of oxygen bonded to the metal and the formation of $Cr(OH)_3$. The corresponding relative fractions of the chemical species are shown in insets of Figures 4d and 5c.

Moreover, as O-1s spectra point out, a non-negligible amount of hydroxyde or hydroxyl groups is present for example as $Cr(OH)_3$ on the surface of both specimens, (i.e. around 46 % OH^- species no matter the type of sample, Figures 4d and 5c). The presence of a considerable amount of these types of species on the surface of both alloys is of great importance because they could significantly contribute to the hydrophilic character of the surface, evidenced from static contact angle measurements. The hydrophilic character of the surface, in terms of surface affinity for the adhesion of the cells, is indispensable for medical applications.

One may conclude that in terms of medical applications, this strategy in adding as alloying elements W and Mo in the CoCr alloy composition is of great perspective in obtaining CoCr -based alloys with lower content of chromium than usually used for such applications.

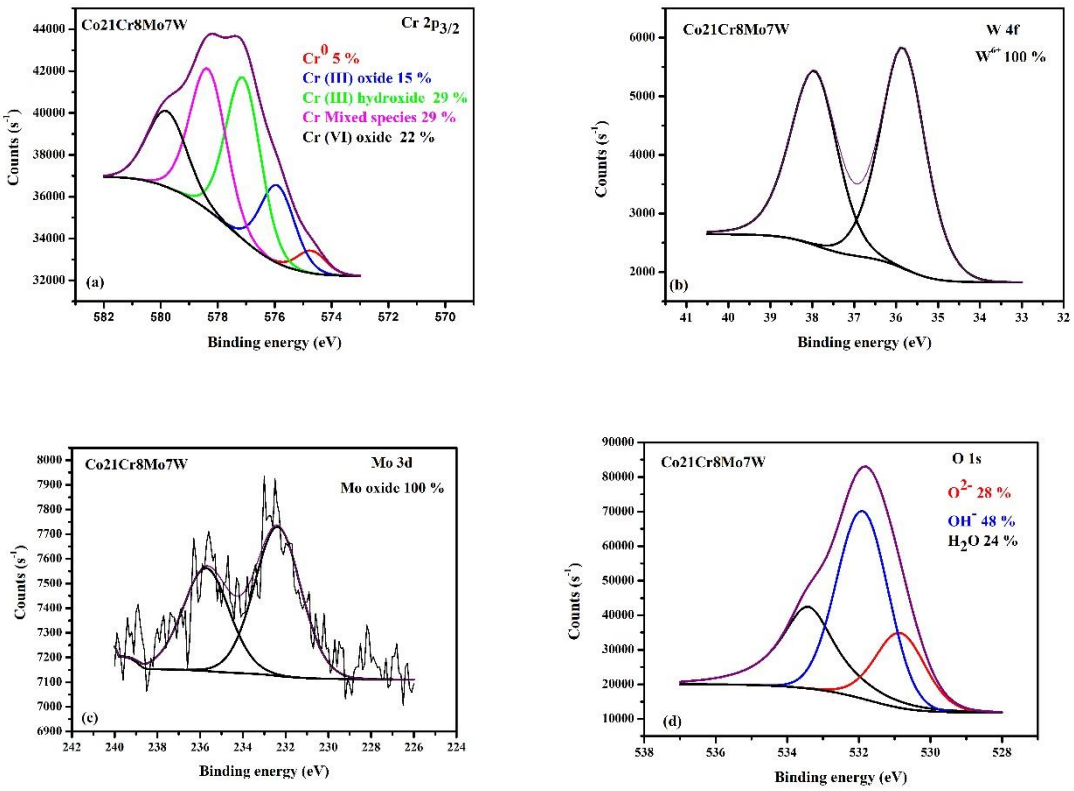

Figure 4. High resolution XPS spectra recorded in the Cr $2p_{3/2}$, W 4f , Mo 3d and O 1s regions for Co21Cr8Mo7W alloy.

Preprints (www.preprints.org) | NOT PEER-REVIEWED | Posted: 10 October 2023 doi:10.20944/preprints202310.0638.v1

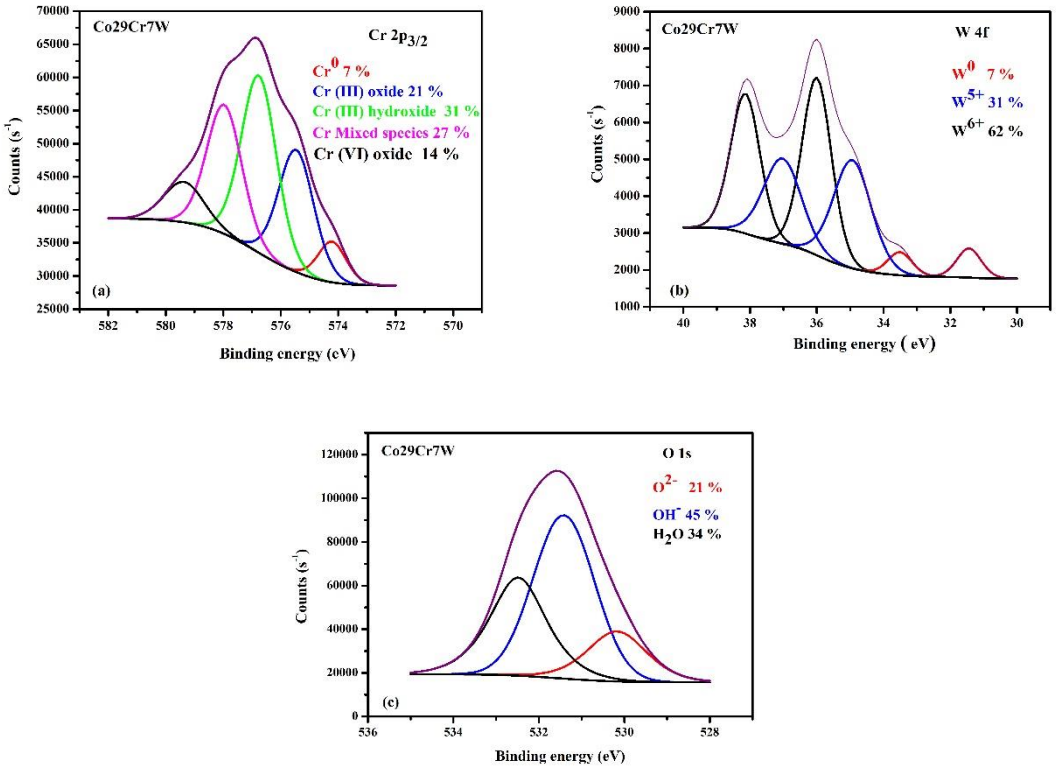

Figure 5. High resolution XPS spectra recorded in the Cr $2p_{3/2}$, W 4f and O 1s regions for Co29Cr7W alloy.

5. Conclusions

The corrosion behavior of two cast CoCr based alloys, one with lower content of chromium (Co21Cr8Mo7W) and another one with higher content of chromium (Co29Cr7W), was systematically investigated in 0.1M PBS, by electrochemical methods, for long period of immersion.

After 1000 hours of immersion, the anodic polarization curves clearly outlined that both studied alloys present good corrosion resistance. Despite the fact that both alloys have similar corrosion behavior, from the estimation of the corrosion parameters, one may resume that Co21Cr8Mo7W alloy has better corrosion protection (i.e. i_{cor} = 49 nA cm^{-2}, E_{cor} = -59 mV and R_{cor} = 2.81 μm y^{-1}) compared to Co29Cr7W alloy (i.e. i_{cor} = 180 nA cm^{-2}, E_{cor} = -114 mV and R_{cor} = 6.57 μm y^{-1}). This behavior attests that on Co21Cr8Mo7W surface a more stable and compact passive film is formed. These outcomes are in line with EIS results which evidenced a higher polarization resistance (R_p) at Co21Cr8Mo7W alloy (i.e. 8.6 M Ω cm^2) compared to Co29Cr7W alloy where a R_p of 3 M Ω cm^2 was determined.

The good corrosion resistance observed at Co29Cr7W, as XPS investigations point, is mainly due to the presence of chromium species (i.e. Cr_2O_3, $Cr(OH)_3$) and tungsten oxide species in the passive film. At Co21Cr8Mo7W, the XPS results suggest that the excellent corrosion behavior of this alloy mainly originates from the synergetic effect of Cr, W and Mo present in the film as Cr_2O_3, $Cr(OH)_3$, WO_3 and MoO_3. Moreover, the present investigations revealed that the presence of a higher amount of Cr_2O_3 and chromium hydroxide species in the film does not necessarily bring about better corrosion performance of these CoCr based alloys. In fact, the remarkable corrosion resistance observed at these CoCr based alloys with a lower content of Cr, namely Co21Cr8Mo7W, emerges, as stated previous, from the strategy of adding different alloying elements (i.e. Mo and W in the CoCr alloy composition.

Additionally, as the ion release measurements suggest, at Co21Cr8Mo7W a low concentration of chromium ion release (i.e. 0.15 μg cm^{-2}), very much beneath the value accepted medical, was evidenced whereas at Co29Cr7W, a high concentration of chromium ion release (i.e. 73.7 μg cm^{-2}), very much over value accepted medical, is observed.

These results are promising ones in terms of medical applications, because the Co21Cr8Mo7W alloy, herein studied, could be regarded as a valid alternative when aiming to develop new CoCr-based alloys for such applications. By using such type of alloy for surgical applications, with lower amount of Cr, new surgical devices with low costs and safely in terms of chromium ion release could be obtained.

Author Contributions: L. P.—Methodology, Conceptualization, Writing-Review; S. A. L.—Investigation; C. D.-Investigation and Formal Analysis; E. I. N.—Investigation; M. E. M.—Investigation; V. S.—Investigation; A. P.—Investigation, M. M.—Conceptualization, Writing—Review, Supervision. All authors have read and agreed to the published version of the manuscript.

Acknowledgments: This study was performed within the framework of the *Electrochemical preparation and characterization of active materials with predetermined features* research project of the „Ilie Murgulescu" Institute of Physical Chemistry of the Romanian Academy.

Conflicts of Interest: The authors declare that they have no known competing financial interest or personal relationships that could have appeared to influence the work reported in this paper.

References

1. Dobri, G.; Banu, A.; Donath, C.; Marcu, M. The Influence of the Tantalum Content on the Main Properties of the TixTa9Nb8Zr2Ag Alloy. *Metals* **2023**, 13, 1294. https://doi.org/10.3390/met13071294
2. Wanga, Q.; Eltit, F.; Fenge, R.; Garbuz, D.; Duncan, C.; Masri, B.A.; Greidanus, N.; Coxc, M.E.; Wanga, R. Nature of fretting corrosion products in CoCrMo hip implants from in vivo study to in vitro simulation. *Materialia* **2022**, 22, 101433. doi.org/10.1016/j.mtla.2022.101433
3. Acharya, S.; Soni, R.; Suwas, S.; Chatterjee, K. Additive manufacturing of Co–Cr alloys for biomedical applications: A concise review. *J. of Mater. Res.* **2021**, 36, 3746-3760. Doi.org/10.1557/s43578-021-00244-z
4. Mazumder, S.; Man, K.; Radhakrishnan, M.; Pantawane, M.V.; Palaniappan, S.; Patil, S.M.; Yang, Y.; Dahotre, N.B. Microstructure enhanced biocompatibility in laser additively manufactured CoCrMo biomedical alloy, *Biomater Adv.* 150 (2023) 213415. https://doi.org/10.1016/j.bioadv.2023.213415 1
5. Mace, A.; Khullar, P.; Bouknight, C.; Gilbert, J.L. Corrosion properties of low carbon CoCrMo and additively manufactured CoCr alloys for dental applications. *Dent. Mater*. **2022**, 38 (7):1184-1193. DOI:10.1016/j.dental.2022.06.021
6. Yan, Y.; Neville, A.; Dowson, D.; Williams, S. Tribocorrosion in implants—Assessing high carbon and low carbon Co–Cr–Mo alloys by in situ electrochemical measurements. *Tribol. Int*. **2006**, 39, 1509. doi:10.1016/j.triboint.2006.01.016
7. España, F. A.; Balla, V.K.; Bose, S.; Bandyopadhyay, A. Design and fabrication of CoCrMo alloy based novel structures for load bearing implants using laser engineered net shaping. *Mater. Sci. Eng. C* **2010**, 30, 50–57. doi.org/10.1016/j.msec.2009.08.006
8. Yamanaka, K.; Mori, M.; Kuramoto, K.; Chiba, A. Development of new Co-Cr-E based biomedical alloys: Effects of micro alloying and thermo mechanical processing on microstructures and mechanical properties. *Mater. Des.* **2014**, 55, 987-998. doi.org/10.1016/j.matdes.2013.10.052
9. Igual, M.A.; Mischler, S. Interactive Effects of Albumin and Phosphate Ions on the Corrosion of CoCrMo Implant Alloy. *J. Electrochem. Soc.* **2007,** 154 , 10, C562-C570. DOI: 10.1149/1.2764238
10. Vidal,V.C.; Igual, M.A. Effect of physico-chemical properties of simulated body fluids on the electrochemical behaviour of CoCrMo alloy. *Electrochim. Acta* **2011**, 56, 8239–8248. doi:10.1016/j.electacta.2011.06.068
11. Banu, A.; Marcu, M.**;** Juganaru, C.; Osiceanu, P.; Anastasescu, M.; Capra, L. Corrosion behavior of CoCrMoW cast alloy in lactic environment. *Arab. J. Chem.* **2019**,12, 2007-2016. DOI: 10.1016/j.arabjc.2017.06.003
12. Metikos-Hukovic', M.; Pilic', Z.; Babic', R.; Omanovic, D. Influence of alloying elements on the corrosion stability of CoCrMo implant alloy in Hank's solution. *Acta Biomater.* **2006**, 2, 93–700. doi:10.1016/j.actbio.2006.06.002
13. Milosev, I.; Strehblow, H.-H. The composition of the surface passive film formed on CoCrMo alloy in simulated physiological solution. *Electrochim. Acta* **2003**, 48, 2767-2774. DOI:10.1016/S0013-4686(03)00396-7
14. Garcia-Falcon, C.M.; Gil-Lopez, T.; Verdu-Vazquez, A.; Mirza-Rosca, J. Electrochemical characterization of some cobalt base alloys in Ringer solution, *Mater. Chem. Phys.* **2021**, 260, 124164. doi.org/10.1016/j.matchemphys.2020.124164
15. Wang, R.; Qin, G.; Zhang, E. Hot deformation characteristics and dynamic recrystallization of biomedical CoCrWCu alloy. *Mater. Today Commun.* **2022**, 33, 104930. doi.org/10.1016/j.mtcomm.2022.104930

16. Tian, W.-P.; Yang, H.-W.; Zhang, S.-De. Synergistic Effect of Mo, W, Mn and Cr on the Passivation Behavior of a Fe-Based Amorphous Alloy Coating. *Acta Metall. Sin. (Engl. Lett.)* **2018,** 31, 308-320. DOI 10.1007/s40195-017-0604-5
17. Cwalina, K.L.; Demarest, C.R.; Gerard, A. Y.; Scully, J.R. Revisiting the effects of molybdenum and tungsten alloying on corrosion behavior of nickel-chromium alloys in aqueous corrosion. *Curr. Opin. Solid State Mater. Sci.* **2019**, 23, 129-141. Doi.org/10.1016/j.cossms.2019.03.002
18. Gurel, S.; Nazarahari, A. Canadinc, D.; Gerstein, G.; Maier, H.J.; Cabuk, H.; Bukulmez, T.; Cananoglu, M.; Yagci, M.B.; Toker, S.M.; Gunes, S.; Soykan, M.N. From corrosion behavior to radiation response: A comprehensive biocompatibility assessment of a CoCrMo medium entropy alloy for utility in orthopedic and dental implants, *Intermetallics* **2022,** 149, 107680. https://doi.org/10.1016/j.intermet.2022.107680
19. Vidal, V.C.; Igual, M.A. Electrochemical characterisation of biomedical alloys for surgical implants in simulated body fluids. *Corros. Sci*. **2008**, 50, 1954-1961. doi:10.1016/j.corsci.2008.04.002
20. Milosev, I. The effect of biomolecules on the behaviour of CoCrMo alloy in various simulated physiological solutions. *Electrochim. Acta* **2012**, 78, 259-273. doi.org/10.1016/j.electacta.2012.05.146
21. Hodgson, A.W.E.; Kurz, S.; Virtanen, S.; Fervel, V.; Olsson, C-O. A.; Mischler, S. Passive and transpassive behaviour of CoCrMo in simulated biological solutions. *Electrochim. Acta* **2004**, 49, 2167-2178. doi:10.1016/j.electacta.2003.12.043
22. Tanawana, T.; Hiromoto, S.; Asami, K. Characterization on of the surface oxide film of a Co-Cr-Mo alloy after being located in quasi-biological environments using XPS. *Appl. Surf. Sci.* **2001,** 183, 68-75. doi.org/10.1016/S0169-4332(01)00551-7
23. Ouerd, A.; Alemany-Dumont, C.; Normand, B.; Szunerits, S. Reactivity of CoCrMo alloy in physiological medium: Electrochemical characterization of the metal/protein interface. *Electrochim. Acta* **2008**, 53, 4461–4469. doi.org/10.1016/j.electacta.2008.01.025
24. Girao, D.de C.; Beres, M.; Jardini, A.L.; Filho, R.M.; Silva, C.C.; Siero. A.; Gomes de Abreu, H.F.; Araujo, W.S. An assessment of biomedical CoCrMo alloy fabricated by direct metal laser sintering technique for implant applications. *Mater. Sci. Eng. C Mater. Biol. Appl.* **2020,** 110305. doi: 10.1016/j.msec.2019.110305
25. Banu, A.; Radovici, O.; Marcu, M. The alloying influence on corrosion behavior of chromium surgical alloys. *Rev. Roum. Chim*. **2008**, 53, 947-953.
26. ISO 10271 Dentistry- Corrosion test methods for metallic materials. ISO: Geneva, Switzerland, **2011**
27. Okazaki, Y.; Gotoh, E. Comparison of metal release from various metallic biomaterials in vitro. *Biomaterials* **2005**, 26, 11–21. doi:10.1016/j.biomaterials. 2004.02.005
28. Spataru, T.; Preda, L.; Munteanu, C.; Caciuleanu, A.; Spataru, N.; Fujishima, A. Influence of boron-doped diamond surface termination on the characteristics of titanium dioxide anodically deposited in the presence of a surfactant. *J. Electrochem. Soc.* **2015**, 162, H535-H540. DOI: 10.1149/2.0741508jes
29. Marin, E.; Lanzutti, A.; Rondinella, A.; Sordetti, F.; Magnan, M.; Honma, T.; Yoshida, Y.; Zhu, W.; Pezzotti, G.; Fedrizzi, L. Multi-spectroscopic analysis of high temperature oxides formed on cobalt-chrome-molybdenum alloys. *J. Mater.Res. Technol.* **2022**, 20, 3061-3073. https://doi.org/10.1016/j.jmrt.2022.08.071
30. Spataru, T.; Mihai, M. A.; Preda, L.; Marcu, M.; Radu, M. M.; Becherescu, N. D.; Alin Velea, A.; Zaki, M. Y.; Udrea, R.; Satulu, V.; Spataru, N. Enhanced photoelectrochemical activity of WO_3-decorated native titania films by mild laser treatment. *Appl. Surf. Sci.* **2022**, 153682. https://doi.org/10.1016/j.apsusc.2022.153682
31. Marcu, M.; Preda, L.; Vizireanu, S.; Bita, B.; Mihai, M. A.; Spataru, T.; Acsente, T.; Dinescu, G.; Spataru, N. Enhancement of the capacitive features of WO_3 supported on pristine and functionalized graphite by appropriate adjustment of the electrodeposition regime. *Mater. Sci. Eng. B* **2022**, 277, 115585. https://doi.org/10.1016/j.mseb.2021.115585
32. Vasilopoulou, M.; Soultati, A.; Georgiadou, D.G.; Stergiopoulos, T.; Palilis, L.C.; Kennou, S.; Stathopoulos, N.A.; Davazoglou, D.; Argitis, P. Hydrogenated understoichiometric tungsten oxide anode interlayers for efficient and stable organic photovoltaics. *J. Mater. Chem. A* **2014**, 2,1738. doi.org/10.1039/ c3ta13975a
33. Alexander, M. R. ; Thompson, G. E.; Zhou, X.; Beamson, G.; Fairley, N. Quantification of oxide film thickness at the surface of aluminium using XPS. *Surf. Interface Anal.* **2002**, 34, 485-489, doi.org/10.1002/sia.1344
34. Preda, L.; Spataru, N.; Moreno, J. M. C.; Somacescu, S.; Marcu, M. Graphene Incorporation as a Propitious Approach for Improving the Oxygen Reduction Reaction (ORR) Activity of Self-assembled Polycrystalline $NiCo_2O_4$–NiO. *Electrocatalysis* **2020**, 11, 443–453. doi.org/10.1007/s12678-020-00605-y